

A VARIABLE SWITCHING FREQUENCY PWM TECHNIQUE FOR INVERTER-FED INDUCTION MOTOR TO ACHIEVE SPREAD SPECTRUM

Binoj Kumar A.C, G. Narayanan

Department of Electrical Engineering
Indian Institute of Science, Bangalore, India

Abstract—Voltage Source Inverter (VSI) fed induction motors are widely used in variable speed applications. For inverters using fixed switching frequency PWM, the output harmonic spectra are located at a few discrete frequencies. The ac motordrives powered by these inverters cause acoustic noise. This paper proposes a new variable switching frequency pwm technique and compares its performance with constant switching frequency pwm technique. It is shown that the proposed technique leads to spread spectra of voltages and currents. Also this technique ensures that no lower order harmonics are present and the current THD is comparable to that of fixed switching frequency PWM and is even better for higher modulation indices.

Index Terms—Harmonic spectra, pulse width modulation, spread spectrum, variable switching frequency pwm (VFPWM)

INTRODUCTION

Electrical drives, especially induction motor drives, play an important role as electromechanical energy converter in industry. Nowadays voltage source inverter (VSI) fed induction motors are widely used in variable speed applications.

Many pulse width modulation (PWM) techniques have been introduced for mitigation of undesirable side effects of harmonics in VSI fed ac drives. In converters with deterministic frequency, the motor generates an unpleasant acoustic switching noise and a mechanical vibration. Also with fixed switching frequency, the harmonic power is concentrated in discrete frequencies of the output voltage. In contrast to that, in converters with spread spectrum, the harmonic spectrum is continuous. The advantage of spreading the spectrum of voltages and currents of the motor is that the acoustic noise produced by the drive can be reduced.

A number of random pulse width modulation (RPWM) strategies have been reported in the literature in order to disperse the switching spectra of induction motor drive. These techniques ignore the presence of low order harmonics in the line to line voltage, and hence the resulting line current distortion is high.

In this paper, a variable frequency PWM technique is proposed to spread the harmonic voltage spectra. At the same time, it is ensured that no lower order harmonics are present in the line to line voltage and the line current THD is comparable to that of conventional space vector PWM (CSVPWM).

CONVENTIONAL SPACE VECTOR PWM

A three phase quantity (voltage or current) can be transformed into a space vector. The components of the space vector along two mutually perpendicular axes (α and β) are defined in (1)

$$\begin{aligned} V_{\alpha} &= \frac{3}{2} V_{RN} \\ V_{\beta} &= \frac{\sqrt{3}}{2} (V_{YN} - V_{BN}) \end{aligned} \quad (1)$$

where V_{RN} , V_{YN} , V_{BN} are line to neutral voltages; V_{α} and V_{β} are the components of the voltage vector along α and β axes.

A. Switching states and voltage vectors of a 2-level VSI

Every leg of the VSI is a single pole double throw (SPDT) switch with the top and bottom devices switching in a complementary fashion. When the top device is ON, the pole voltage measured with respect to the DC bus neutral (point 'O') is $+V_{dc}/2$. When the bottom device is ON, the pole voltage is $-V_{dc}/2$. With three switch legs, there are 2^3 or 8 states possible switching states as shown in Fig.1. For each switching state, the three phase pole voltages (V_{RO} , V_{YO} , V_{BO}) and line to line voltages (V_{RY} , V_{YB} , V_{BR}) are uniquely defined. Assuming a three phase balanced star connected load, the corresponding line to neutral voltages can also be defined.

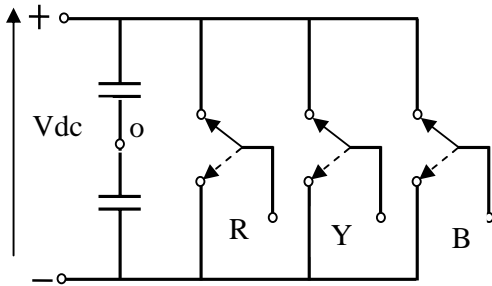


Fig.1. Two-level voltage source inverter

When all the top devices are ON or all the bottom devices are ON, the three phase loads are shorted by the inverter. There is no transfer of power between the DC bus and the three phase load. These two states are termed as zero states of the inverter (+++ and ---). The other states of the inverter are termed as active states, which lead to six active vectors of equal magnitude Vdc. These active vectors divide the space vector plane into six sectors of angle 60° as shown in Fig 2.

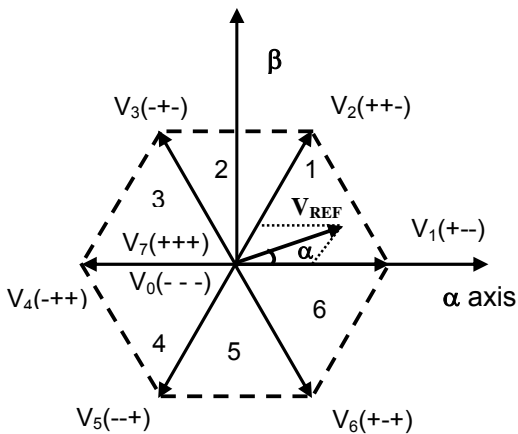


Fig.2. Space vectors of a 2-level voltage source inverter

In space vector based PWM, the voltage reference is provided by a revolving reference vector V_{REF} which is sampled once in every T_s . At steady state, V_{REF} is proportional to the desired fundamental voltage and its frequency equals the fundamental frequency. In fact, V_{REF} represents the average vector to be applied in the given subcycle, and can be best realized by the vectors bounding the sector in which it is present using the principle of volt-second balance as shown below.

$$V_{REF} T_s = V_1 T_1 + V_2 T_2 + V_z T_z \quad (2)$$

where T_s is the subcycle duration, V_1 and V_2 are the active vectors bounding the sector and V_z is the zero vector. T_1 , T_2 and T_z denote the dwell times of the states/vectors and are given by the following expressions.

$$T_1 = \frac{V_{REF} \sin(60 - \alpha) * T_s}{V_{dc} \sin 60}$$

$$T_2 = \frac{V_{REF} \sin \alpha * T_s}{V_{dc} \sin 60} \quad (3)$$

$$T_z = T_s - (T_1 + T_2)$$

The zero vector can be applied either using the zero state 0 or the zero state 7. The switching instants of the three phases depend on the division of T_z between 0 and 7 and the switching sequence employed. Conventional space vector PWM applies both the zero states equally for a duration $T_z/2$ as shown in Fig 3. The sequence of inverter states is 0-1-2-7 (forward sequence) and 7-2-1-0 (reverse sequence) in alternate subcycles in sector I. However, a multiplicity of sequences are possible since the zero vector can be applied either using 0 or 7 and also an active state can be applied more than once in a sub cycle [1].

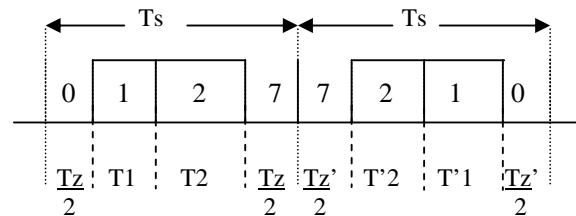


Fig.3. 0-1-2-7 switching sequence of CSVPWM in one switching period (2Ts)

PROPOSED VARIABLE SWITCHING FREQUENCY CSVPWM

In a PWM inverter fed induction motor drive, there is an error between the instantaneous applied voltage vector and the reference voltage vector. For a given reference vector in sector 1, the error voltage vectors corresponding to the active vector 1, the active vector 2 and the zero vector are as illustrated in Fig. 4, and as expressed below.

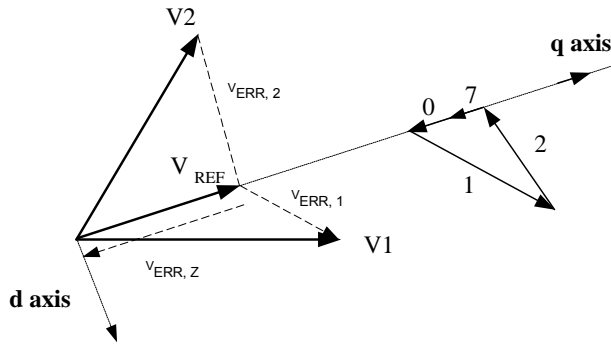


Fig.4. Error voltage vectors corresponding to V_1 , V_2 and V_z

$$\begin{aligned} V_{ERR,1} &= V_1 - V_{REF} \\ V_{ERR,2} &= V_2 - V_{REF} \\ V_{ERR,z} &= -V_{REF}. \end{aligned} \quad (4)$$

The time integral of the error voltage vector is termed here as the “stator flux ripple vector.” For harmonic voltages, an induction motor can simply be modeled by its total leakage inductance. Therefore the integral of the error voltage or the stator flux ripple is proportional to the current ripple (both differ by a factor of leakage inductance). Hence flux ripple is a measure of the ripple in line current. In particular, the rms value of stator flux ripple over a subcycle is a measure of the rms current ripple over the given subcycle.

A. Expression for RMS Flux Ripple

The mean square value of stator flux ripple over a subcycle can be expressed as in (5) [2].

$$\bar{v}^2_{sub} = [c_0 * Vr^2 + c_1(\alpha) * Vr^4 + c_2(\alpha) * Vr^4] Ts^2 \quad (5)$$

$$c_0 = \frac{1}{12}$$

$$c_1 = \frac{3}{3\sqrt{3}} \left[\frac{32}{9} (ab^4 + a^3b^2 - a^2b^3) + \frac{2}{3} (-2b^3 - 3ab^2 - a^2b) + b - a \right]$$

$$c_2 = \frac{1}{9} \left[\frac{4}{3} (a^3b - 2ab^3 - a^2b^2) + a^2 + 4b^2 - 2ab \right]$$

where

$$a = \sin(60 + \alpha)$$

$$b = \sin(60 - \alpha)$$

It is clear from these equations that the rms stator flux (current) ripple over a subcycle depends on the reference vector and T_s .

B. Dependence of Flux Ripple on α

In the rms stator flux ripple expressions, replacing α by $(60^\circ - \alpha)$ is equivalent to interchanging of T_1 and T_2 . Hence the rms flux ripple plotted against α over a sector is symmetrical about $\alpha = 30^\circ$. As seen from Fig. 5, the rms ripple over a subcycle is low when α is close to 0° or 60° . The rms ripple has its peak at $\alpha = 30^\circ$ [1].

Spread spectrum can be achieved by varying the subcycle duration with respect to α over a range which is determined by a factor k . That is, now subcycle duration (T_s) is a function of α and is varied in such a fashion that

- (i) Dispersed frequency spectrum is obtained
- (ii) Rms current ripple is reduced resulting in less current distortion
- (iii) Its variation is symmetrical about $\alpha = 30^\circ$
- (iv) Number of switchings per sector is the same.

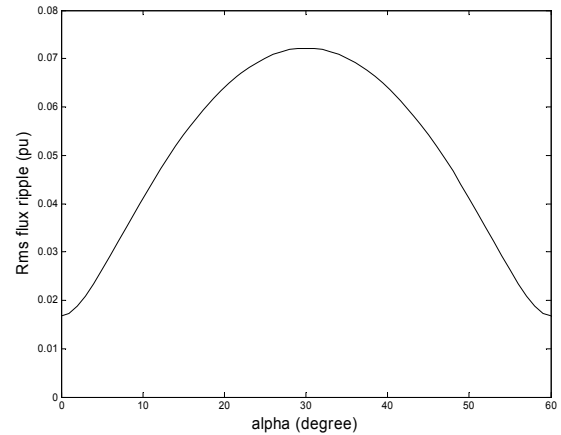


Fig.5. Variation of rms flux ripple with α over a sector

As a simple case, linear variation of $T_s(\alpha)$ is considered over a sector as shown in Fig. 6. Here

$$\begin{aligned} T_{s_{max}} &= (1+k) * T_s \\ T_{s_{min}} &= (1-k) * T_s \end{aligned} \quad (6)$$

so that the average switching period in one sector is T_s . The variation of $T_s(\alpha)$ can be expressed as an equation.

$$\begin{aligned} T_s(\alpha) &= T_s \left[1 + k \left(1 - \frac{12\alpha}{\pi} \right) \right], \quad 0 \leq \alpha \leq \frac{\pi}{6} \\ &= T_s \left[1 - k \left(3 - \frac{12\alpha}{\pi} \right) \right], \quad \frac{\pi}{6} \leq \alpha \leq \frac{\pi}{3} \end{aligned} \quad (7)$$

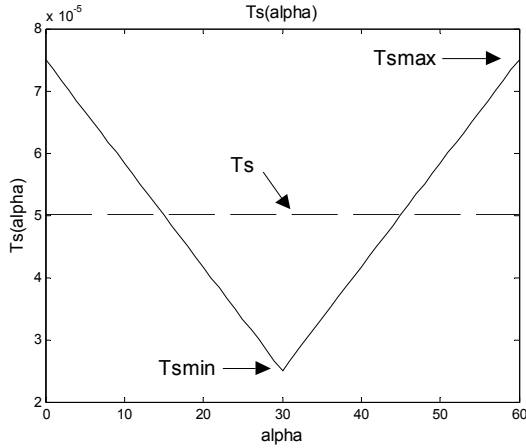


Fig.6. Variation of subcycle time duration, $T_s(\alpha)$ with α over a sector ($f_c = 10$ kHz)

Selection of k depends on the desired spread of harmonic spectrum and V_{REF} . Also range of k is restricted by practical limits. Rms current ripple over a subcycle and its average over a sector are shown in Fig. 7. For a comparison, a fixed switching period ($k=0$) and a variable switching period ($k=0.5$) are used.

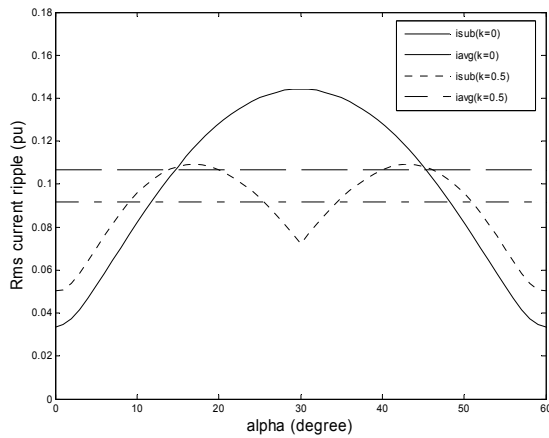


Fig.7. Variation of subcycle rms current ripple and average rms current ripple over a sector with α for $k= 0$ and 0.5 ($V_{REF} = 0.866$)

MODULATING SIGNAL IN CSVPWM

Analog implementation of CSVPWM is possible if the modified references (V_R^* , V_Y^* , V_B^*) are used for determining the switching instants instead of V_R , V_Y and V_B [6]. For that an offset,

$$V_{off} = -0.5*(V_{max} + V_{min}) = 0.5 V_{mid} \quad (8)$$

is used. The common mode component appears almost like a triangular wave of peak equal to 25% of the peak of the modulating sinusoid and frequency equal to three times the fundamental frequency. Addition of this offset voltage to the three phase sinusoidal signals results in the modified modulating waves as shown below.

$$\begin{aligned} V_R^* &= V_R + V_{off} \\ V_Y^* &= V_Y + V_{off} \\ V_B^* &= V_B + V_{off} \end{aligned} \quad (9)$$

EXPERIMENTAL RESULTS

The fixed frequency and variable frequency PWM (VFPWM) techniques are implemented on a digital control platform based on ALTERA Cyclone field programmable gate array (FPGA) device. A 10 kVA IGBT based voltage source inverter is used to feed a 3kW, 200V, 10.5A, 50Hz three phase induction motor.

A. Voltage Harmonic Spectra

The measured harmonic spectra of line-line voltage (PWM of R-phase minus PWM of Y-phase) corresponding to CSVPWM and VFPWM are shown in Fig. 8 to Fig. 13 for a fundamental frequency of 50Hz. The spectra corresponding to CSVPWM have sidebands around f_c , $2f_c$, $3f_c$, etc. For example, in Fig. 8, harmonic spectra are concentrated in sidebands around 4.88kHz, 9.76 kHz, etc. The harmonic spectrum pertaining to VFPWM (Fig. 9) is well dispersed without any dominant harmonic components and no low order harmonics are present. Fig. 10 shows harmonic spectra of the line-line voltage (PWM of R-phase minus PWM of Y-phase) corresponding to CSVPWM for a switching frequency of 9.76 kHz. Discrete harmonic spectra are obtained at 9.76 kHz, 19.5 kHz etc. On the other hand, a spread spectrum is obtained with VFPWM as shown in Fig. 11. The spectra in Fig. 10 and Fig.11 are enlarged for clarity, and are shown in Fig. 12 and Fig. 13. It is clear from these figures that harmonic spectra are dispersed in VFPWM and low order harmonics are also absent.

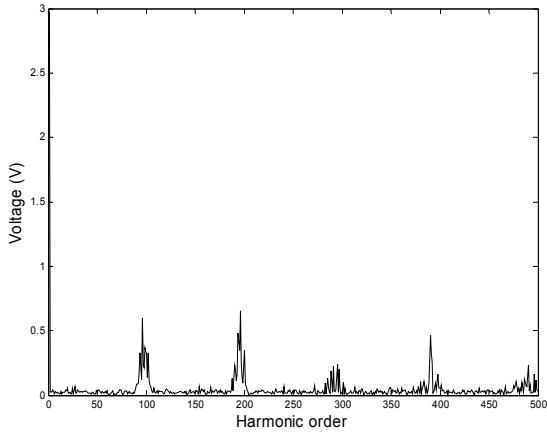


Fig.8. Frequency spectrum of (PWM of R-phase minus PWM of Y-phase) with CSVPWM for $f=50\text{Hz}$ and $f_c = 4.88 \text{ kHz}$ (Experimental result).

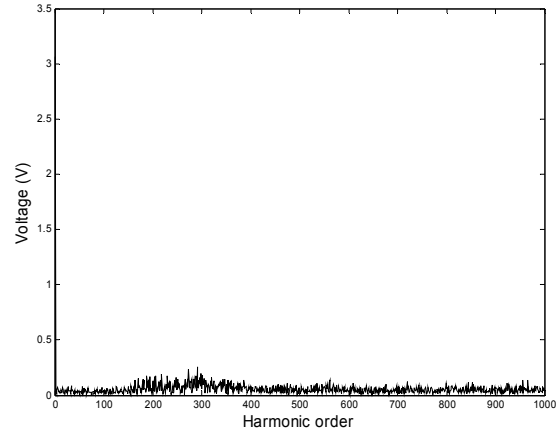


Fig.11. Frequency spectrum of (PWM of R-phase minus PWM of Y-phase) with variable frequency PWM for $k=0.5$ and $f=50\text{Hz}$ (Experimental result).

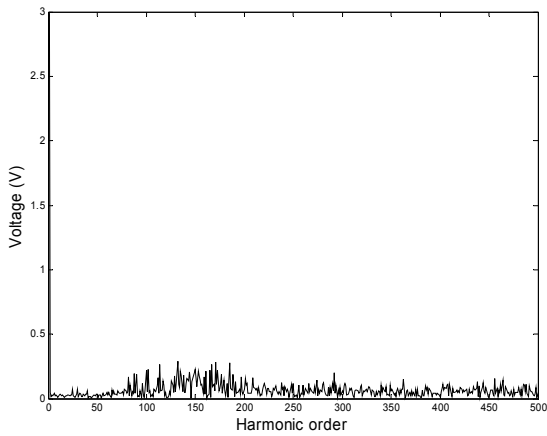


Fig.9. Frequency spectrum of (PWM of R-phase minus PWM of Y-phase) with variable frequency PWM for $k=0.5$ and $f=50\text{Hz}$ (Experimental result)

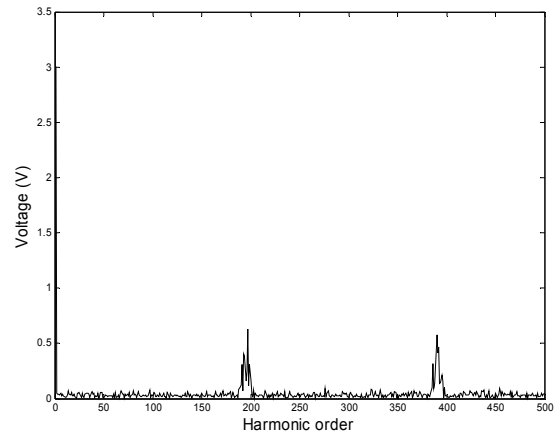


Fig.12. Frequency spectrum of (PWM of R-phase minus PWM of Y-phase) with CSVPWM for $f=50\text{Hz}$ and $f_c = 9.76 \text{ kHz}$ (Experimental result).

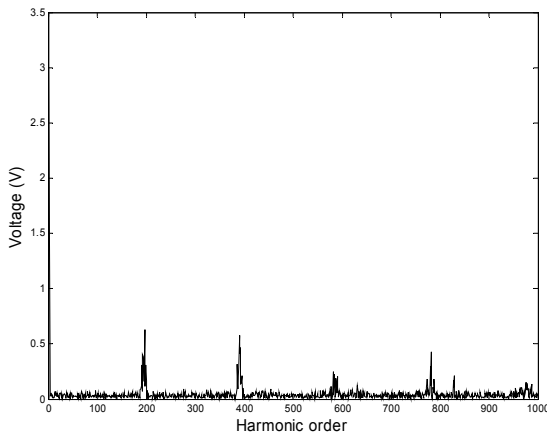


Fig.10. Frequency spectrum of (PWM of R-phase minus PWM of Y-phase) with CSVPWM for $f=50\text{Hz}$ and $f_c = 9.76 \text{ kHz}$ (Experimental result).

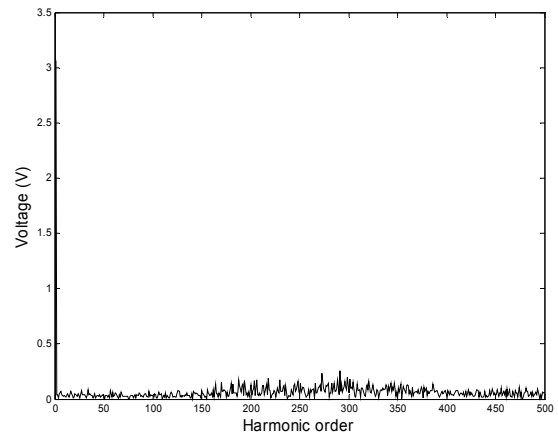


Fig.13. Frequency spectrum of (PWM of R-phase minus PWM of Y-phase) with variable frequency PWM for $k=0.5$ and $f=50\text{Hz}$ (Experimental result).

B. No-load Motor Current

Measured no-load current waveforms pertaining to CSVPWM and VFPWM techniques are shown in Fig. 14 and Fig. 15, respectively. Current THD in motor no-load current with CSVPWM technique is 10.78% whereas the same with VFPWM technique is 10.14% at 50 Hz. Fig. 16 and Fig. 17 show the frequency spectra of motor line current with CSVPWM and VFPWM, respectively. It can be seen that with CSVPWM, the harmonics is concentrated around sidebands of 2.44 kHz, 4,88 kHz etc. But a distributed spectrum is obtained for VFPWM without much low order harmonics.

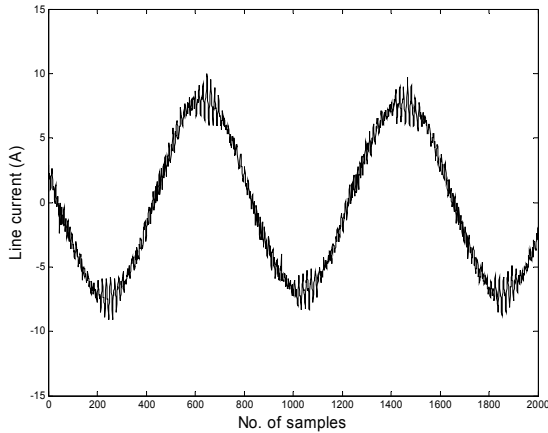


Fig.14. Measured motor no-load current with CSVPWM for $f=50\text{Hz}$ and $f_c=2.44\text{ kHz}$ (Experimental result). The measured current THD is 10.78%

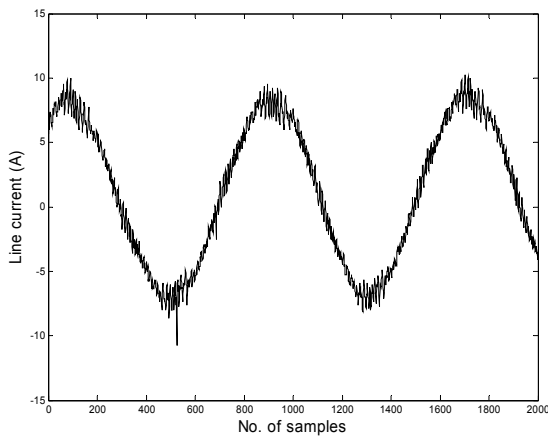


Fig.15. Measured motor no-load current with variable frequency PWM for $k=0.5$ and $f = 50\text{Hz}$ (Experimental result). The measured current THD is 10.14%

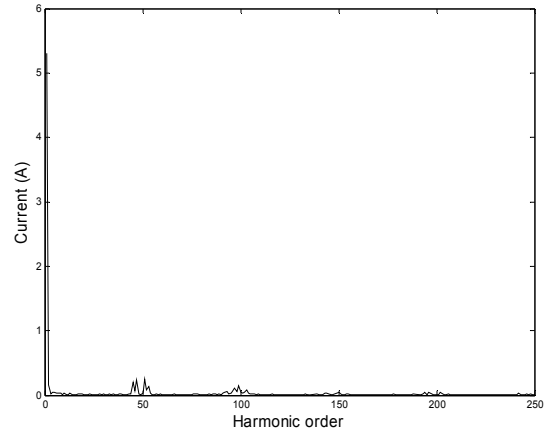


Fig.16. Frequency spectrum of line current with CSVPWM for $f=50\text{Hz}$ and $f_c = 2.44\text{ kHz}$. (Experimental result).

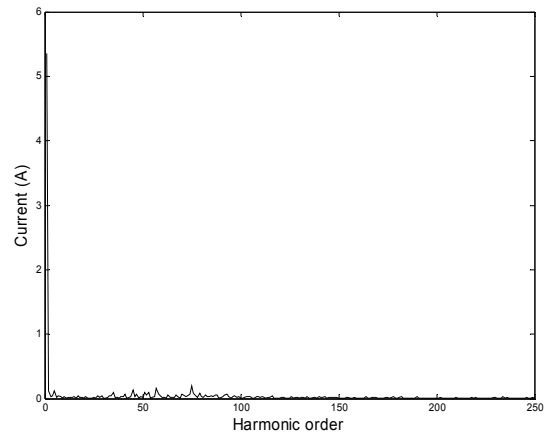


Fig.17. Frequency spectrum of line current with variable frequency PWM for $k=0.5$ and $f=50\text{Hz}$ (Experimental result).

CONCLUSION

Voltage source inverters are widely used to provide power to induction motors, which are the main workhorse of industry. In CSVPWM, a carrier signal of constant frequency is compared with the modulating signal to generate the desired PWM signals. The proposed technique based on variable frequency carrier signal could achieve spread spectrum of voltages and currents. At the same time, no lower order harmonics are present in the line to line voltage and the line current THD is comparable to that of CSVPWM and is even better for higher modulation indices.

REFERENCES

- [1] G. Narayanan, Di Zhao, Harish K. Krishnamurthy, Rajapandian Ayyanar and V. T. Ranganathan, "Space Vector Based Hybrid PWM Techniques for Reduced Current Ripple," *IEEE Trans. Ind. Electron*, vol. 55, no. 4, pp.1614-1627, Apr. 2008
- [2] Di Zhao, V. S. S. Pavan Kumar Hari, G.Narayanan, Rajapandian Ayyanar, "Space-Vector-Based Hybrid Pulsewidth Modulation Techniques for Reduced Harmonic Distortion and Switching Loss," *IEEE Trans. Power Electron.*, vol. 25, no. 3, pp. 760-774, Mar. 2010.
- [3] L. Mathe, P. O. Rasmussen, J. K. Pedersen, "Shaping the spectra of the line-to-line voltage using signal injection in the common mode voltage," in *Proc. Ind. Electron. Conf. 2009 (IECON'09)*, pp. 1288-1293, Nov. 2009.
- [4] A. M. Trzynadlowski, F. Blaabjerg, J. K. Pedersen, R. L. Kirlin, and S. Legowski, "Random pulse width modulation techniques for converter fed drive systems—A review," *IEEE Trans. Ind. Appl.*, vol. 30, no. 5, pp. 1166–1174, Sep./Oct. 1994.
- [5] Ki-Seon Kim, Young-Gook Jung, and Young-Cheol Lim, "A New Hybrid Random PWM Scheme," *IEEE Trans. Power Electron.*, vol. 24, no. 1, pp. 192-200, Jan. 2009.
- [6] P Srikant Varma and G Narayanan, "Space Vector PWM as a modified form of Sine-triangle PWM for simple Analog or Digital implementation," *IETE Journal of Research*, vol.52, no.6, pp. 435-449, Nov-Dec 2006.



G. Narayanan received the B.E. degree from the Anna University, Chennai, in 1992, and the M.Tech degree from the Indian Institute of Technology, Kharagpur, in 1994. He received the PhD degree from the Indian Institute of Science, Bangalore, in 2000, where he is currently an Associate Professor in the Department of Electrical Engineering. His research interests include ac drives, pulse width modulation, multilevel inverters and protection of power devices.

Dr. Narayanan received the Innovative Student Project Award for his PhD work from the Indian National Academy of Engineering in 2000, and the Young Scientist Award from the Indian National Science Academy in 2003.



Binoj Kumar A.C. received the B.Tech degree from Rajiv Gandhi Institute of Technology, Kottayam, Kerala, in 1998 and the M.Tech degree from College of Engineering, Thiruvananthapuram, Kerala, in 2001. He is currently pursuing the PhD degree at the Department of Electrical Engineering, Indian Institute of Science, Bangalore. His research interests include pulse width modulation techniques and electrical drives.